Int. J. Electrochem. Sci., 11 **(2016)** 7764 – 7774, doi: 10.20964/2016.09.22

International Journal of
ELECTROCHEMICAL
SCIENCE
www.electrochemsci.org

Short Communication

Corrosion Resistance of Inconel 625 Overlay Welded Inside Pipes as a Function of Heat Treatment Temperature

So-dam Ban[1], *Young-Taek Shin*[2], *Sung Riong Lee*[3], *Hae-woo Lee*[1,*]

[1] Department of Materials Science and Engineering, Dong-A University, Busan Rep. of Korea
[2] Department of Naval Architecture and Offshore Engineering, Dong-A University, Busan, Rep. of Korea.
[3]Departmnet of Materials and Metallurgical Engineering, Kangwon National University, Kangwon-do, Rep. of Korea.
[*]E-mail: hwlee@dau.ac.kr

Received: 1 June 2016 / *Accepted:* 12 July 2016 / *Published:* 7 August 2016

The effect of the heat treatment temperature on the corrosion resistance and precipitation of weld overlaid Inconel 625 has been investigated. Gas metal arc welding was performed using Inconel 625 as a filler metal with the ASTM A333Gr 6.The heat treatment was carried out on test specimens at 650℃, 750℃, 850℃, and 950℃ for 24 hours. After heat treatment, the microstructure and elemental composition was investigated. At 650℃, the specimen showed a dendritic pattern, and secondary phases was observed, whereas the fine γ''-phase observed at 750℃. At 850℃, the δ-phase was clearly observed, which was dissolved in the matrix at 950℃ and no longer visible. In addition, potentiodynamic polarization tests were performed to evaluate the pitting corrosion resistance. The results confirmed that there were no significant differences between the specimens. Double loop electrochemical potentiokinetic reactivationtests were undertaken to characterize the sensitization against intergranular corrosion. These results clearly showed that no sensitization occurred at any of the heat-treatment temperatures tested here.

Keywords: Inconel 625,Gas metal arc welding, overlay, potentiodynamic test, DL-EPR test

1. INTRODUCTION

Ni-based alloys have excellent corrosion resistance and mechanical strength to withstand highly corrosive and high temperature environments, such as in petrochemical, marine, and crude oil and gas industries. The addition of elemental Cr, Cu, Mo, Nb, Fe, and W has been reported to enhance the pitting corrosion resistance and mechanical properties of the Ni-based alloys for various applications. The common Ni-alloy brands include Monel, Inconel, Hastelloy, etc. [1-3].

Inconel 625 is a solid solution strengthening type alloy that is mainly composed of Ni-Cr-Mo-Nb elements where Mo increases the overall corrosion resistance, Cr improves the high temperature oxidation resistance, and Nb reduces intergranular corrosion by forming carbides. This alloy has been widely used in the aerospace, marine, and nuclear industries since it exhibits excellent corrosion resistance, mechanical properties, and weldability at both intermediate and high temperatures. However, the practical application of Inconel 625 is still limited due to its high cost. To overcome this problem, thin sheets of Inconel 625 have recently been overlay welded onto lower cost carbon steel or low-alloy steel to provide the excellent corrosion resistance at a reduced production cost [4-10].

Inconel 625 was initially produced as a solid solution strengthening alloy, but it shows precipitation, intermetallic compounds, and carbide formation at specific temperatures and over time. In the temperature range of 600–700°C, there is no change in the microstructure. But at temperatures higher than 700°C, the γ”(Ni_3Nb) phase appears along the interdendritic regions. This precipitate hardens the alloy is metastable and has a body-centered tetragonal structure. At temperatures between around 850–950^{0}C, the γ”-phase dissolves into the bulk and the δ(Ni_3Nb) phase forms. As the aging temperature increases, the metastable γ”-phase changes into the orthorhombic δ-phase.[11,12] Previous studies[13] have shown that the formation of the γ”-phase improves the strength, while the δ-phase reduces the strength and ductility. Although the ductility recovers at temperatures of approximately 1000°C and above, as the δ-phase dissolves and becomes homogenized, the strength still decreases due to the crystal grain growth. Also, at specific temperatures and times, the intermetallic laves phase compounds and the MC, M_6C, and $M_{23}C_6$ type carbides precipitate. In spite of having high mechanical strength and corrosion resistance, the laves and δ phases of Inconel 625 which precipitate during long welding at high temperatures reduce the toughness, fatigue strength, and creep rupture strength of the welds [14-22].

It has been revealed[11] that at temperatures above 600°C, different precipitates could be formed depending on the temperature range. Thus, when the alloy is exposed to high temperatures in an aerospace engine or nuclear fusion plant, the microstructure of the material will change. In this paper, an Inconel 625 filler metal was gas metal arc welded inside a carbon steel pipe. The test specimens were heated for 24 hours at temperatures of 650℃, 750℃, 850℃, and 950℃.The microstructures and precipitates at each temperature were analyzed and the corrosion properties at different temperatures were determined.

2. EXPERIMENTAL METHODS

2.1 Welding and specimen preparation

In this study, the overlay welding was conducted using the gas-metal arc welding (GMAW) method. An ASTM A333 Grade 6 carbon steel pipe was used as the base material and the Inconel

625(UNS N06625-NiCr22Mo9Nb) was used as the filler metal. The specimens were prepared as illustrated in Fig.1. The welding conditions and the compositions of the A333 Grade 6 pipe and Inconel 625 areshown in Table 1 and Table 2, respectively. Table 3 shows the weld composition of the prepared specimens.

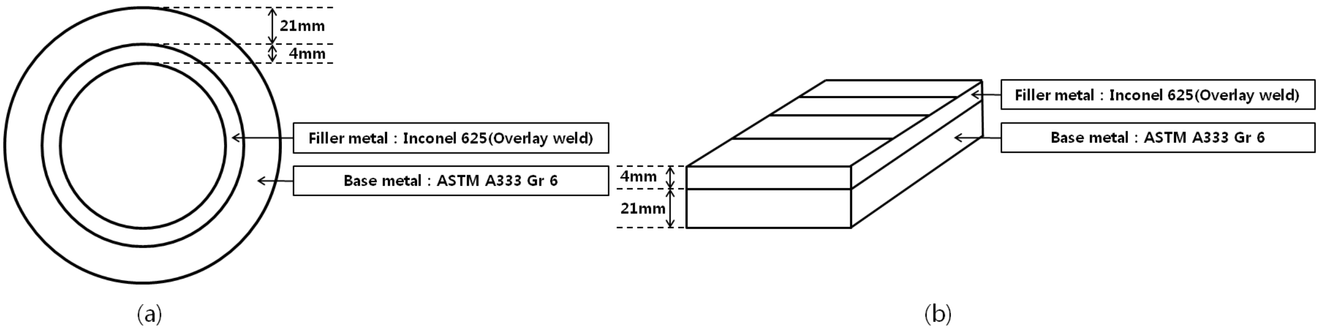

Figure 1. Specimen geometry (a) Inconel 625 overlay welded pipe, (b) each specimen for tests

Table 1. Welding conditions (wt.%)

Filler Metal	Current(A)	Voltage(V)	Welding Speed (cm/min)	Feed Rate (cm/min)
Inconel 625	193	14	19.6	105

Table 2. Composition of A333 Gr 6 base metal and Inconel 625 filler metal (wt.%)

	C	Mn	Si	Cr	Ni	Mo	Nb	Fe	Ti
A333 Gr 6	0.18	0.94	0.19	0.09	0.06	-	-	98.4	-
Inconel 625	0.01	0.01	0.04	22.24	64.8	8.73	3.54	0.27	0.17

Table 3. Composition of weld (wt.%)

	C	Mn	Si	Cr	Ni	Mo	Nb	Fe	Ti
Inconel 625 welding layer	0.023	0.07	0.08	20.21	60.5	8.01	3.73	5.18	0.18

2.2 Heat treatment conditions

The time-temperature-precipitation curve of the Inconel 625alloy is shown in Fig. 2[11]. Based on this data, the specimens were subjected to heat treatment at 650℃, 750℃, 850℃, and 950℃ for 24 hours in order to obtain the different precipitates corresponding to different zones (i.e. temperatures) of the welding area.

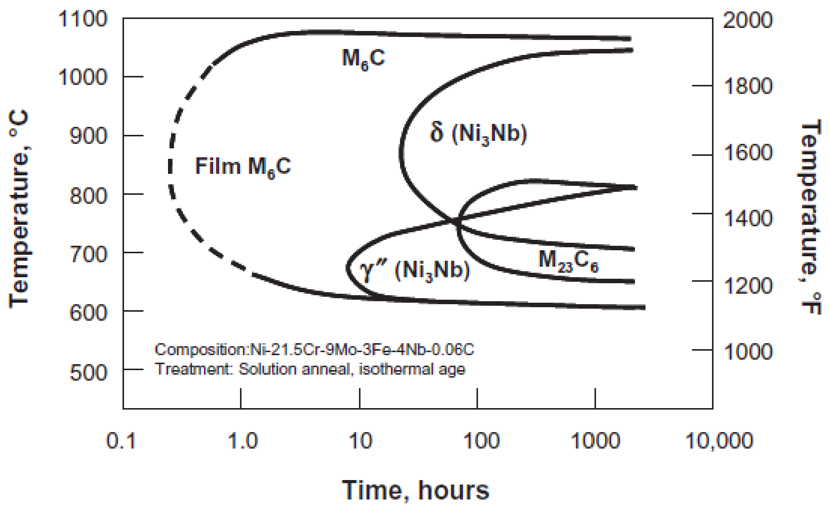

Figure 2. Time-temperature-precipitation diagram showing the different precipitate phases of an Inconel 625.

2.3 Characterization of the weld

In order to characterize the structure of each weld, silicon carbide paper(SIC) abrasive paper was used for #600 to #1200 grinding and 1µm, 3µmpolishing. All specimens were then etched with aqua regia, a3:1 mixture hydrochloric acid (HCl) and nitric acid (HNO_3) [5]. After etching, the microstructures and the elemental composition of the precipitates were analyzed using scanning electron microscopy(SEM) and energy dispersive X-ray spectroscopy(EDS) JEOL JSM-6700F. The microstructure was observed on the surface of the overlay welds. Also, transmission electron microscope(TEM) JEOL JEM-2010 is used to observe γ”. The specimen was prepared to thickness of 800µm and cut it into 3mm diameter. Then jet polishing was conducted in containing 5% perchloric acid and 95% Methyl Alcohol at -15℃ and 34V. It took for 20 to 30 seconds.

2.4 Electrochemical testing

2.4.1 Pitting corrosion resistance

Potentiodynamic polarization tests were conducted on the specimens treated at different temperatures to investigate the pitting corrosion resistance. The specimens with an area of1 cm^2were polished with #1200-grid SIC abrasive paper and then washed. A VersaSTAT 3potentiostat/galvanostat (Princeton Applied Research) was used for the corrosion test with aK0235

Flat Cell three-electrode system (with thespecimen as the working electrode, Ag-AgCl/saturated KCl as the reference electrode, and platinum foil as the counter electrode). To determine the corrosion properties of the Inconel 625alloy under simulated seawater conditions, a 3.5% NaCl solution was used during the polarization tests. All testswere conducted with aninitial electrode potential of -0.5mV, a final potential of -0.5mV and a scan rate of 0.5mV/sec at room temperature.

2.4.2 Intergranular corrosion resistance

In order to measure the sensitization of the samples to intergranular corrosion, the double loop electrochemical potentiokinetic reactivation(DL-EPR) test was performed. The same VersaSTAT 3 equipment and electrochemical cell as described for the potentiodynamic polarization tests were used. Referring to International Standard ISO12732 [26], the test was carried out in 2M H_2SO_4 + 2M HCl + 0.01M KSCN solution at 25℃. Before conducting the experiment, the open circuit potential was applied for 20 minutes in order to form a stable passive film on the specimen surface. The DL-EPR test was then carried out with an initial potential of -0.5mV, vertex potential of 0.8mV, and final potential of -0.5mV at a scan rate of 0.5mV/s. The intergranular corrosion resistance was determined by measuring the degree of sensitization(DOS) from the ratio of the maximum anode current density when the potential increases (l_a) and the maximum anode current density when the current decreases (l_r).

3. RESULTS AND DISCUSSION

3.1 Microstructure

Figs. 3 (a)-(d) show SEM images of the specimens after heat treatment at 650℃, 750℃, 850℃, or 950℃ for 24 hours. The specimen treated at 650℃ showed a microstructure (Fig. 3a) composed of secondary phases along the interdendritic area. The microstructure of the specimen heat-treated at 750℃ showed fine γ”-phase was observed along the interdendritic area (Fig. 3b). Fig. 4a shows TEM image of the γ”-phase on the matrix(γ) and diffraction pattern. The dislocations are concentrated around γ” precipitations. Large spot is $[001]_{fcc}$ of γ-matrix and fine spot is γ” pattern. Shape of precipitations appears clearly at the dark field image (Fig. 4b). Xixuexing, et al. [12] reported that the rectangular metastable precipitates form at the initial stage of the γ- phase growth. As temperature increases, the corners of the rectangular γ”-phase dissolve into the γ matrix resulting in irregular, short, and long rectangular structures. Additionally, depending on the temperature increase, the body-centered tetragonal γ” phase could transform into the needle-shaped prismatic δ-phase due to the lattice strain. At 850℃, the γ” phase almost disappears completely, and the δ-phase formation along the interdendritic area can be clearly seen, compared to the 750℃ sample (Fig. 3c).On the δ-phase, intermetallic compounds containing a large amount of Nb and Mo is observed by EDS (Fig. 4c). At 950℃, most of the γ” and δ-phase had disappeared. Meanwhile, some of the δ phase and smaller particles of carbides containing Nb and Mo observed (Fig. 4d).

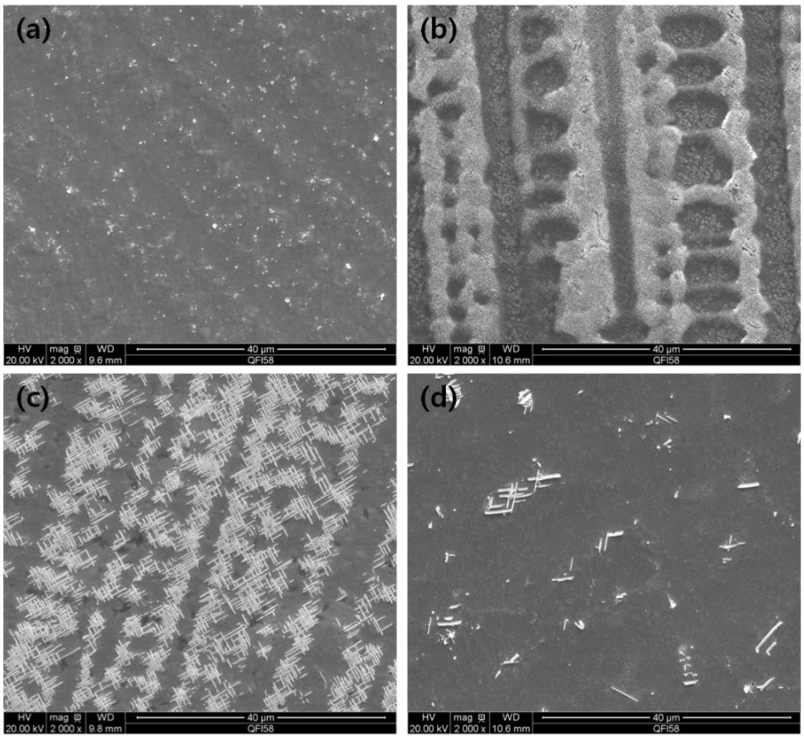

Figure 3. Microstructure of weld metal after heat treatment for 24 hours at (a) 650℃, (b) 750℃, (c) 850℃, and (d) 950℃

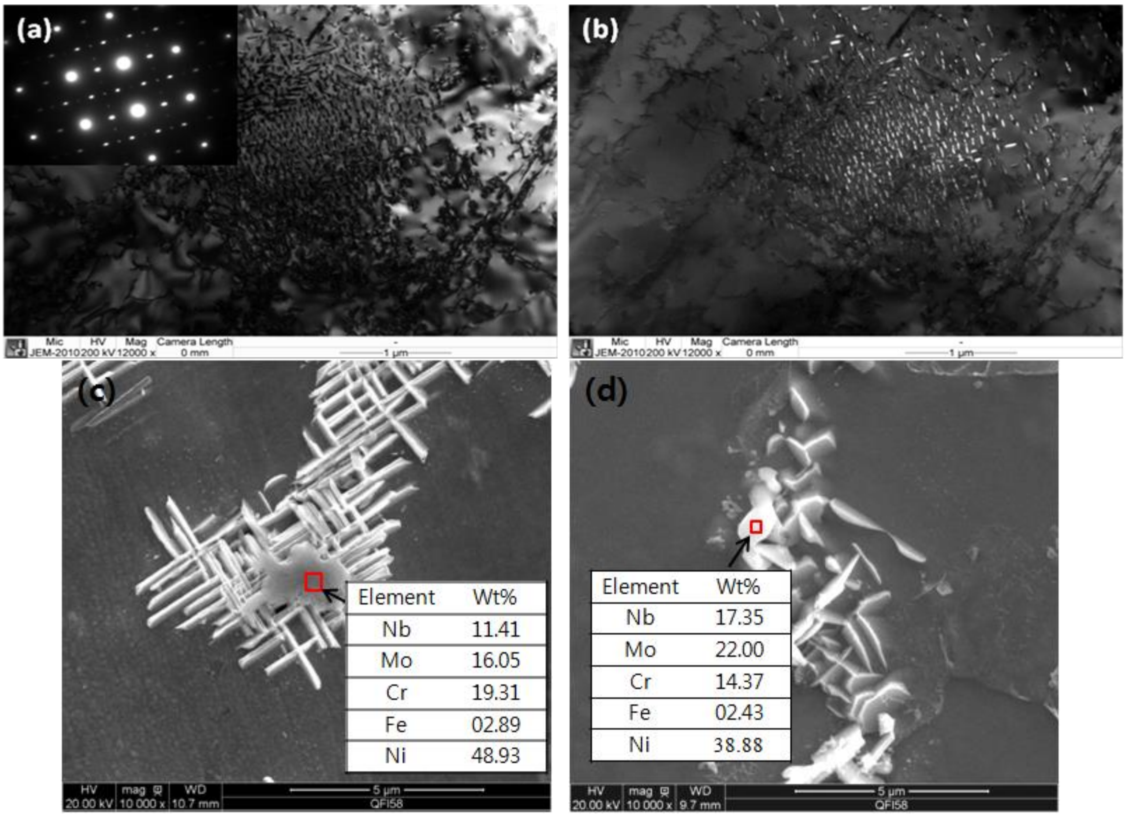

Figure 4. Precipitates on the weld metal after heat treatment 24hours (a) bright field image with the diffraction pattern of matrix$[011]_{fcc}$ and γ” at 750℃, (b) dark field image of (a), (c) 850℃ and (d) 950℃

3.2 Electrochemical properties

3.2.1 Pitting corrosion resistance

The results of the potentiodynamic polarization tests to evaluate the pitting corrosion resistance of the Inconel 625samples heat-treated at different temperatures are shown in Fig. 5. Using the Tafel extrapolation method, the value of the corrosion potential (E_{corr}), pitting potential (E_{pit}), passive region (ΔE), and corrosion current (I_{corr}) were determined, and are shown in Table 4. At 850℃, both E_{corr} and E_{pit} had the lowest values. However, at 650℃, 750℃, and 950℃, the values showed a similar trend. The passive region is obtained by subtracting E_{pit} from E_{corr}. The larger the passive region(ΔE) is, the more stable a passive film is. At 850℃, the ΔE is also the smaller the others. In this graph, the pitting potentials are appeared at 650℃, 750℃, 850℃, and 950℃.but there is no pitting corrosion at all temperatures when the surface after this tests is observed by SEM (Fig. 6). Corrosion products consisting of Nb, Mo and O formed on the surface after potentiodynamic tests. SEM/EDS mapping was carried out to know elements of corrosion products in Fig. 7. The corrosion mechanism is known as galvanic coupling that the dendritic matrix serves as sacrificial anode[23]. The corrosion product is considered that a large amount of Nb and Mo is formed compounds with O.

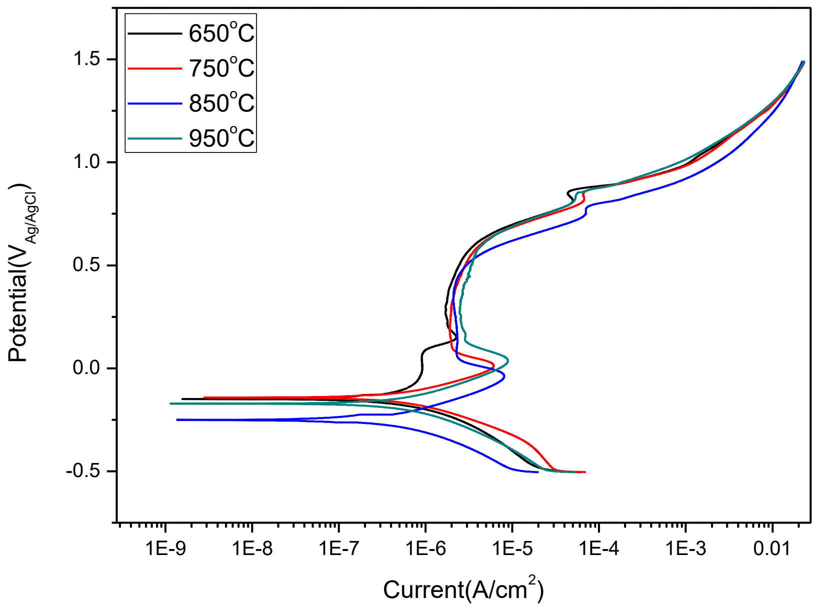

Figure 5. Potential versus current density curves from potentiodynamic polarization tests of samples heat-treated for 24 hours at 650℃, 750℃, 850℃, or 950℃

Table 4. Corrosion parameters of the potentiodynamic polarization tests in a 3.5% NaCl solution

	650℃	750℃	850℃	950℃
E_{corr} (mV)	-149.1	-142.1	-249.7	-171.8
E_{pit} (mV)	637.0	619.5	487.0	585.2
ΔE (mV)	786.2	761.7	736.7	756.9
I_{corr} (nA)	973.5	691.0	367.3	732.8

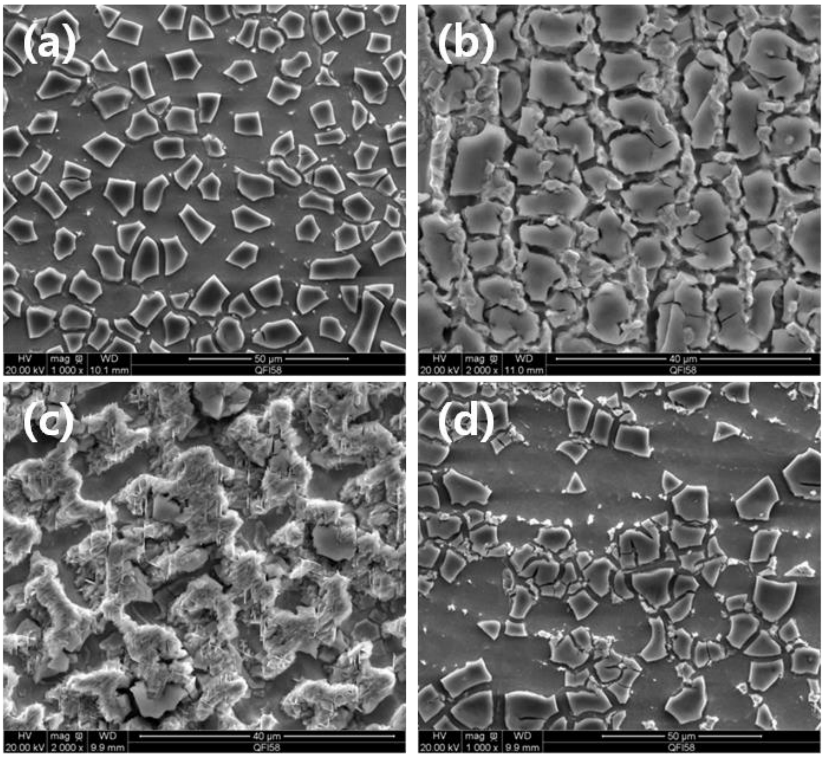

Figure 6. Scanning electron micrographs of specimens heat-treated at (a) 650℃, (b) 750℃, (c) 850℃ and (d) 950℃ after potentiodynamic tests

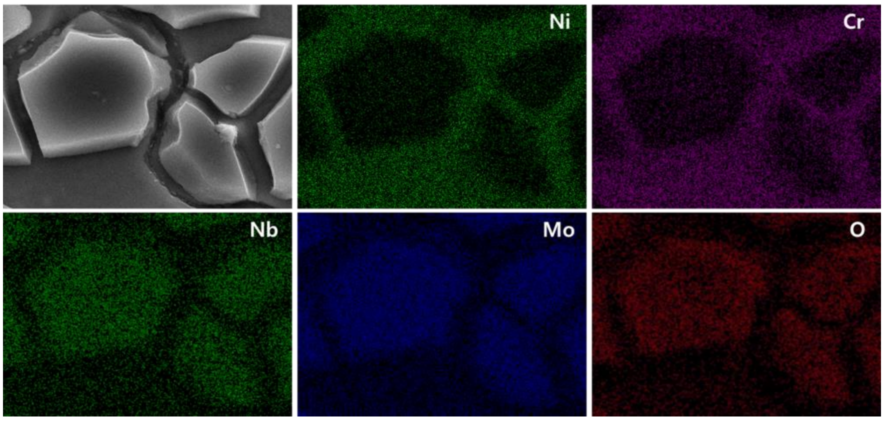

Figure 7. SEM/EDS mapping of the specimen surface at 650℃ after potentiodynamic tests

3.2.2 Intergranular corrosion test

The results of the DL-EPR tests performed to determine the intergranular corrosion resistance of the Inconel 625samples heat-treated at different temperatures are shown in Fig.8. The values of I_a, I_r, and I_r/I_a, that are related to the degree of sensitization, are listed in Table 5. It can be concluded that if I_a and I_r have similar values, the sensitization has progressed considerably. However, here the I_a and I_r values are significantly different and hence the sensitization effect is minor [24]. Lippold et al. [11] reported that the resistance to intergranular corrosion at temperatures between 700℃ and 950℃ is reduced due to the existence of γ” and δ phases. At temperatures higher than 950℃, the intergranular corrosion resistance increases as the γ” and δ phases are dissolved. In this study, the highest value for the maximum anode current density on the anode curve was found at 850℃, while the lowest value was at 750℃. In the reverse curve, the highest value of the maximum anode current density was found at 750℃, while the lowest wasat 850℃. The degree of sensitization for 650℃, 750℃, 850℃, and 950℃ was 0.007, 0.014, 0.003, and 0.009, respectively. According to ISO 12732, when the degree of sensitization is higher than or equal to 0.05, sensitization can occur [25]. In this study, the degree of sensitization at all temperatures is less than 0.05. In Fig.9, the surface corrosion as characterized by SEM is shown. It was found that corrosion did not occur at 650^{0}C, even though carbides formed along the grain boundaries. In addition, no intergranular corrosion was observed at other temperatures.

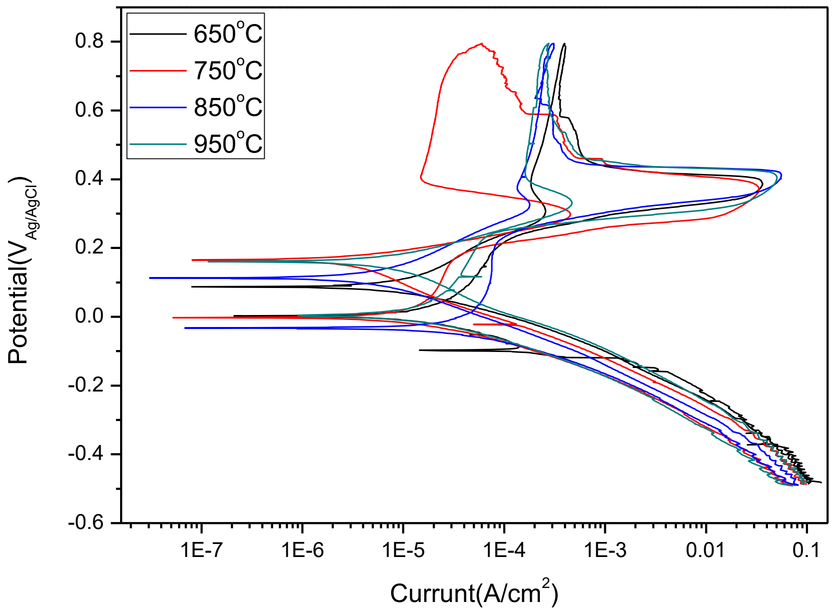

Figure 8. Potential versus current density curves obtained from DL-EPR tests on samples heat-treated for 24 hours at 650℃, 750℃, 850℃, or 950℃

Table 5. Degree of sensitization of the samples heat-treated at different temperatures

	I_a (mA)	**I_r (μA)**	**I_r/I_a**
650℃	34.7	256.0	0.007
750℃	31.0	442.5	0.014
850℃	51.5	175.3	0.003
950℃	47.7	429.7	0.009

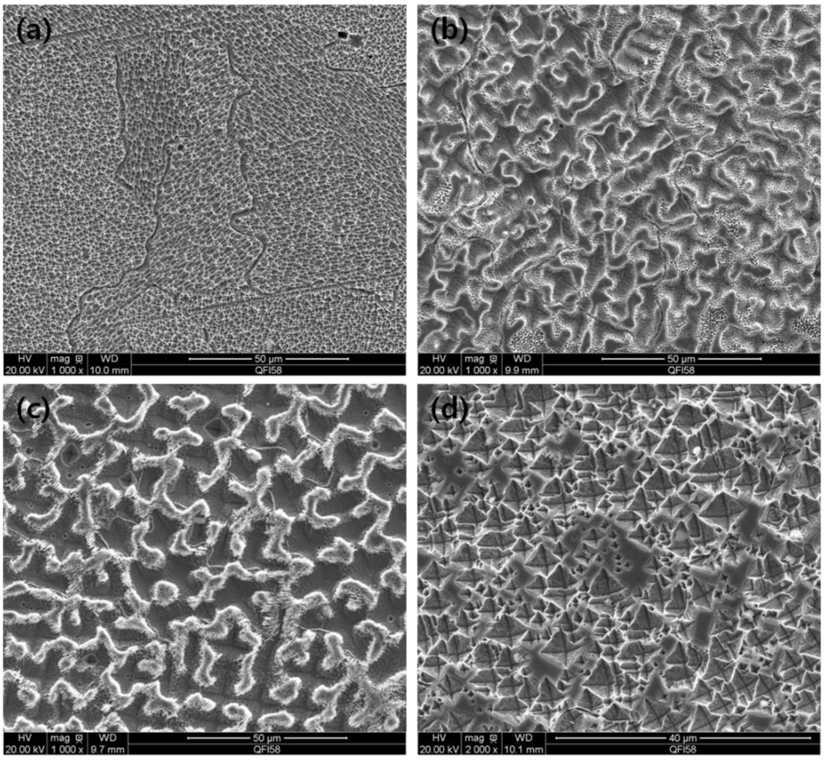

Figure 9. Scanning electron micrographs of specimens heat-treated at (a) 650℃, (b) 750℃, (c) 850℃ and (d) 950℃ after DL-EPR tests

4. CONCLUSION

The corrosion properties of Inconel 625 overlays welded onto carbon steel were determined by performing microstructural and electrochemical tests on samples heat-treated at 650℃, 750℃, 850℃, and 950℃. The following conclusions can be made from this study.

1) At 650℃, a dendritic microstructure and secondary phases along the interdendritic area were observed, while at 750℃ the γ″-phase were found at the interdendritic area. At 850℃,the δ-phase could be clearly observed in the interdendritic region, together with intermetallic compounds containing a large amount of Nb and Mo. At 950℃, the δ phase is dissolved into the matrix structure, and carbides containing a large amount of Nb and Mo were seen in most of the matrix.

2) The results of the potentiodynamic polarization test in a 3.5% NaCl solution revealed that the corrosion potential, pitting potential, and the width of the passive region were the lowest for the sample heat-treated at 850℃. The pitting resistance potential difference between the specimens prepared at different temperatures was insignificant and pitting corrosion was not observed.

3) The sensitization was measured using the DL-EPR test with an intergranular corrosion test method with a 2M H_2SO_4 + 2M HCl + 0.01M KSCN solution. No sensitization was observed for any of the temperatures tested (the DOS values of all samples were less than 0.05).

4) Thus, it can be concluded that there is no relationship between the observed precipitates at different heat treatment temperatures and the corrosion behavior for the samples and conditions tested here.

ACKNOWLEDGEMENT
This investigation was supported by the Dong-A University Research Fund.

References

1. Z. F. Yin, W. Z. Zhao, W. Y. Lai, and X. H. Zhao, *Corros. Sci.,* 51(8) (2009) 1702.
2. Y. -S. Yoo, *Korean Indus. Chem. News,* 17(4) (2014) 1.
3. L. Tan, X. Ren, K. Sridharan and T. R. Allen, *Corros. Sci.,* 50(11) (2008) 3056.
4. P. Ganesan, C. M. Renteria, and J. R. Crum. *Superalloys,* 718 (1991) 625.
5. L. Ferrer, B. Pieraggi, and J. F. Uginet, Proceedings of the Int. Symp. on the Metallurgy and Applications of Superalloys 718, 625 and Various Derivatives(E. A. Louria), p. 217-228, TMS., New York (1991)
6. H. M. Tawancy, *J. Mater. Sci. Lett.,* 11(21) (1992) 1446.
7. M. Rozmus-Górnikowska, L. Cieniek and M. Blicharski, *Arch. Metall. Mater.,* 59(3) (2014) 1081.
8. H.-C. Yoo, *J. KWJS,* 31(1) (2013) 17.
9. C. C. Silva, H. C. de Miranda, M. F. Motta, J. P. Farias, C. R. M. Afonso and A. J. Ramirez, *J. Mater. Res. Technol.,* 2(3) (2013) 228.
10. S. Hassan, Ph. D. Thesis, p. 19-36, University of Nottingham, Nottingham (2011)
11. J. C. Lippold, S. D. Kiser and J. N. DuPont, *Welding Metallurgy and Weldability of Nickel-Base Alloys,* 1st ed., p. 1-206, John Wiley & Sons Inc., Hoboken, New Jersey, USA (2011).
12. X. Xing, D. Xinjie and W. Baosen, *J. Alloy. Compd.,* 593 (2014) 110.
13. V. Shankar, K. Bhanu, S. Rao, and S. L. Mannan, *J. Nucl. Mater.,* 288(2) (2001) 222.
14. H.M. Tawancy, I. M. Allam, and N. M. Abbas, J. Mater. Sci. Lett., 9(3) (1990) 343.
15. L. M. Suave, D. Bertheau, J. Cormier, P. Villechaise, A. Soula, Z. Hervier, F. Hamon and J. Laigo, 8th International Symposium on Superalloy 718 and Derivatives, 1st ed., p. 317-331, John Wiley & Sons Inc.-TMS, Hoboken, New Jersey, USA (2014).
16. J. Mittra, S. Banerjee, R. Tewari and G. K. Dey, Mat. Sci. Eng. A, 574 (2013) 86.
17. V. Číhal and R. Štefec. *Electrochim. Acta,* 46(24) (2001) 3867.
18. M. J. Cieslak, R. J. Headley, A. D. Romig and T. Kollie, *Metall. Trans. A, 19*(9) (1988), 2319.
19. M. Sundararaman, P. Mukhopadhyay, and S. Banerjee., *Metall. Trans. A,* 19(3) (1988) 453.
20. X. Zhang, X. Xie, Z. Yang, J. Dong, Z. Xu, Y. Gao and T. Zhang, *Surf. Coat. Technol.,* 131(1) (2000) 378.
21. M. C. Maguire and J. R. Michael, 3rd Int. Special Emphasis Symp. on Superalloys 718, 625, 706 and Various Derivatives(E. A. Louria), p. 881-892, TMS., Pittsburg, PA (1994).
22. J.J. Kai, G. P. Yu, C. H. Tsai, M. N. Liu and S. C. Yao, *Metall. Trans*. A, 20(10) (1989) 2057.
23. T. E. Abioye, D. G. McCartney and A. T. Clare, *J. Mater. Pro. Tech*., 217 (2015) 232.
24. M. Prohaska, H. Kanduth, G. Mori, R. Grill and G. Tischler, *Corros. Sci.,* 52(5) (2010) 1582.
25. Corrosion of metals and alloys-Electrochemical potentiokinetic reactivation measurement using the double loop method (based on Čihal's method), British Standard, ISO 12732:2008. 2008.